Target Detection Algorithms in Hyperspectral Imaging Based on Discriminant Analysis

Edisanter Lo
Susquehanna University, Selinsgrove, Pennsylvania, USA
Email: loe@susqu.edu

***Abstract*—Target detection algorithm in hyperspectral imaging detects a certain material in a hyperspectral image using a known spectral signature of the material. Conventional algorithms for target detection assume that there is only one known target spectrum so target statistics cannot be estimated. Discriminant analysis is designed for classification, but this paper analyzes the performance of discriminant functions for target detection. The discriminant functions have been modified for target detection and uses simulated target spectra with different amount of random noise. Experimental results show that the algorithms can work well within a certain amount of noise.**

***Index Terms*—target detection, hyperspectral imaging, remote sensing**

I. Introduction

Hyperspectral imaging forms images of a scene by using an imaging spectrometer to collect the reflectance spectrum of each pixel in the scene. The spectrum covers a wide range of wavelengths. Hyperspectral images have high spectral resolution and has hundreds of spectral bands. The main applications of hyperspectral imaging in remote sensing are target detection, anomaly detection, and classification. Different materials have different spectral signatures. Target detection uses a known spectral signature from an image or spectral library to detect a specific material in the image from the spectrum of the pixel. Target detection assumes the image consists of only background pixels and target pixels. Unlike classification, which requires a sample of training pixels for the background and a sample of training pixels for the target, target detection requires a sample of training pixels for the background and only one training pixel for the target.

The papers in [1], [2] give a review of target detection algorithms for hyperspectral imaging. The conventional algorithms Adaptive Matched Filter (AMF) in [3] and Adaptive Coherence/Cosine Angle (ACE) in [4] are commonly used in target detection. A recent review of AMF and ACE is in [5]. An algorithm based on logistic regression for target detection is in [6], and this algorithm uses simulated target pixels for training the detector. A constrained ACE detector for highly variable target is presented in [7], [8], and these algorithms implant simulated target pixels as test pixels. Other approaches to target detection are discussed in [9]-[11].

Both the AMF and ACE assume the background pixels and target pixels form multivariate normal distributions. The AMF assumes a common population covariance Σ for both the background and target distributions. The AMF is derived from a general likelihood ratio test and is given by

$$d_{amf}(x) = \frac{s^T \hat{\Sigma}^{-1} x}{s^T \hat{\Sigma}^{-1} s} \tag{1}$$

where $\hat{\Sigma}^{-1}$ is the inverse of the sample covariance $\hat{\Sigma}$, s is a target spectrum, and x is a test pixel. The mean is removed from the target spectrum and all pixels in image.

ACE is derived from the general likelihood ratio test. The null hypothesis tests if the test pixel has a normal distribution with mean 0 and covariance Σ. The alternative hypothesis tests if the test pixel has a normal distribution with mean as and covariance $\sigma^2\Sigma$. The vector s is the known target spectrum, and σ^2 and a are unknown scalars. The ACE detector for a test pixel x is given by

$$d_{ace}(x) = \frac{\left(x^T \hat{\Sigma}^{-1} s\right)\left(s^T \hat{\Sigma}^{-1} s\right)^{-1}\left(s^T \hat{\Sigma}^{-1} x\right)}{x^T \hat{\Sigma}^{-1} x} \tag{2}$$

This paper proposes to modify the linear discriminant and quadratic discriminant functions for target detection and compare their performance under different noise level. There is usually one target pixel available in target detection so additional training pixels for target need to be generated. The target training pixels are generated by adding a small perturbation to the mean target pixel. The source of the target spectral signature can be from the image, field measurements, or laboratory measurements. Experimental results using the mean target pixel from the image is presented in this paper.

II. Detection Algorithms

A. Bayes' Theorem for Target Detection

The linear discriminant and quadratic discriminant functions are classification methods that produce a binary outcome. The two discriminant functions are modified below for target detection to produce an image of detector

Manuscript received July 1, 2019; revised November 8, 2019.

doi: 10.18178/joig.7.4.140-144

output. The detector output is defined as the value of the modified linear discriminant or modified quadratic discriminant function.

Let the random vector X of dimensions $p\times 1$ and scalar random variable Y represent a test pixel and class, respectively. A value x of the test pixel X is to be classified as a background pixel $(Y=b)$ or target pixel $(Y=t)$. Let the prior probability of a test pixel being a background pixel, density function of X for a test pixel that is a background pixel, prior probability of a test pixel being a target pixel, and density function of X for a test pixel that is a target pixel be denoted by, respectively,

$\pi_b = P(Y=b)$, $f_b(x) = P(X=x/Y=b)$, $\pi_t = P(Y=t)$, and $f_t(x) = P(X=x/Y=t)$.

The Bayes' theorem states the probability that a given test pixel is a background pixel is

$$P(Y=b/X=x) = \frac{\pi_b f_b(x)}{\pi_b f_b(x) + \pi_t f_t(x)} \quad (3)$$

and the probability that a given test pixel is a target pixel is

$$P(Y=t/X=x) = \frac{\pi_t f_t(x)}{\pi_b f_b(x) + \pi_t f_t(x)} \quad (4)$$

A test pixel is classified as a target pixel if

$$\frac{\pi_t f_t(x)}{\pi_b f_b(x) + \pi_t f_t(x)} > \frac{\pi_b f_b(x)}{\pi_b f_b(x) + \pi_t f_t(x)} \quad (5)$$

B. Linear Discriminant for Target Detection

Assume the background pixel and target pixel come from multivariate normal distributions with mean μ_b and covariance Σ_b for the background pixel and mean μ_t and covariance Σ_t for the target pixel. The density functions for the background pixel and target pixel are given by

$$f_b(x) = \frac{\exp\left(-\frac{1}{2}(x-\mu_b)^{'}\Sigma_b^{-1}(x-\mu_b)\right)}{(2\pi)^{p/2}|\Sigma_b|^{1/2}} \quad (6)$$

$$f_t(x) = \frac{\exp\left(-\frac{1}{2}(x-\mu_t)^{'}\Sigma_t^{-1}(x-\mu_t)\right)}{(2\pi)^{p/2}|\Sigma_t|^{1/2}} \quad (7)$$

The linear discriminant analysis does not require the covariance of the target by assuming the background and target have a common covariance matrix, i.e. $\Sigma_b = \Sigma_t = \Sigma$. Assuming that the prior probabilities are equal, Equation (5) can written as

$$f_t(x)/f_b(x) > 1 \quad (8)$$

The density functions in (8) can be replaced by (6) and (7) to obtain the inequality

$$\frac{\exp\left(-\frac{1}{2}(x-\mu_t)^{'}\Sigma^{-1}(x-\mu_t)\right)}{\exp\left(-\frac{1}{2}(x-\mu_b)^{'}\Sigma^{-1}(x-\mu_b)\right)} > 1 \quad (9)$$

By combining the exponential terms and then taking the natural log on both sides, Equation (9) becomes

$$(x-\mu_b)^{'}\Sigma^{-1}(x-\mu_b) - (x-\mu_t)^{'}\Sigma^{-1}(x-\mu_t) > 0 \quad (10)$$

The detector based on linear discriminant analysis for target detection is defined as the left side of (10), i.e.

$$d_L(x) = (x-\mu_b)^{'}\Sigma^{-1}(x-\mu_b) - (x-\mu_t)^{'}\Sigma^{-1}(x-\mu_t) \quad (11)$$

By multiplying out the products, (11) becomes

$$\begin{aligned} d_L(x) = {} & \left(x^{'}\Sigma^{-1}x - x^{'}\Sigma^{-1}\mu_b - \mu_b^{'}\Sigma^{-1}x + \mu_b^{'}\Sigma^{-1}\mu_b\right) \\ & -\left(x^{'}\Sigma^{-1}x - x^{'}\Sigma^{-1}\mu_t - \mu_t^{'}\Sigma^{-1}x + \mu_t^{'}\Sigma^{-1}\mu_t\right) \end{aligned} \quad (12)$$

By adding a zero term $\mu_t^{'}\Sigma^{-1}\mu_b - \mu_b^{'}\Sigma^{-1}\mu_t$ to (12) and then simplifying it, (12) becomes

$$\begin{aligned} d_L(x) = {} & 2\left(\mu_t^{'}\Sigma^{-1}x - \mu_b^{'}\Sigma^{-1}x\right) - \\ & \left(\mu_t^{'}\Sigma^{-1}\mu_t + \mu_t^{'}\Sigma^{-1}\mu_b - \mu_b^{'}\Sigma^{-1}\mu_t - \mu_b^{'}\Sigma^{-1}\mu_b\right) \\ = {} & 2(\mu_t-\mu_b)^{'}\Sigma^{-1}x - (\mu_t-\mu_b)^{'}\Sigma^{-1}(\mu_t+\mu_b) \end{aligned} \quad (13)$$

The second term in (13) does not depend on the test pixel x. A large value of the detector would indicate a target pixel. Target detection typically assumes target pixels are rare so the common covariance Σ can be estimated by the sample covariance $\hat{\Sigma}$ computed using all pixels from the image. The means μ_b and μ_t can be estimated using the sample means $\hat{\mu}_b$ and $\hat{\mu}_t$.

C. Quadratic Discriminant for Target Detection

The quadratic discriminant analysis assumes that the background and target have different covariance matrices, i.e. $\Sigma_b = \Sigma_t$. The covariance for the background can be estimated using the background pixels. There is typically only one known target pixel to be used as the target spectral signature so additional target pixels are needed to estimate the sample mean and sample covariance for the target. The additional target pixels are generated by adding a uniform random noise to the known target pixel.

The density functions in (8) can be replaced by (6) and (7) to obtain the following

$$\left(|\Sigma_b|/|\Sigma_t|\right)^{1/2}\frac{\exp\left(-Q_t/2\right)}{\exp\left(-Q_b/2\right)}>1 \tag{14}$$

$$\begin{aligned} Q_b &= \left(x-\mu_b\right)'\Sigma_b^{-1}\left(x-\mu_b\right) \\ Q_t &= \left(x-\mu_t\right)'\Sigma_t^{-1}\left(x-\mu_t\right) \end{aligned} \tag{15}$$

Equation (14) can be simplified to

$$\exp\left(-\left(Q_t-Q_b\right)/2\right)>\left(|\Sigma_t|/|\Sigma_b|\right)^{1/2} \tag{16}$$

By taking the natural log on both sides of the equation, (16) becomes

$$Q_t-Q_b>\ln\left(\frac{|\Sigma_t|}{|\Sigma_b|}\right) \tag{17}$$

The right side of (17) is not a function of x. Define the left side of (17) as the detector based on quadratic discriminant analysis for target detection, i.e.

$$d_Q\left(x\right)=Q_b-Q_t \tag{18}$$

By multiplying out the products, (18) becomes

$$\begin{aligned} d_Q\left(x\right)=&\left(-x'\Sigma_b^{-1}\mu_b-\mu_b'\Sigma_b^{-1}x+\mu_b'\Sigma_b^{-1}\mu_b\right) \\ &-\left(-x'\Sigma_t^{-1}\mu_t-\mu_t'\Sigma_t^{-1}x+\mu_t'\Sigma_t^{-1}\mu_t\right) \end{aligned} \tag{19}$$

Equation (19) can be simplified to the following final version of the detector

$$\begin{aligned} &d_Q\left(x\right)=-x'\left(\Sigma_t^{-1}-\Sigma_b^{-1}\right)x+ \\ &2\left(\mu_t'\Sigma_t^{-1}-\mu_b'\Sigma_b^{-1}\right)x-\left(\mu_t'\Sigma_t^{-1}\mu_t-\mu_b'\Sigma_b^{-1}\mu_b\right) \end{aligned} \tag{20}$$

A large value of the detector would indicate a target pixel. The means μ_b and μ_t and covariances Σ_b and Σ_t can be estimated using the corresponding sample means $\hat{\mu}_b$ and $\hat{\mu}_t$ and sample covariances $\hat{\Sigma}_b$ and $\hat{\Sigma}_t$.

III. Experimental Results

To The objective of the experiment is to assess the performance of the linear discriminant analysis and quadratic discriminant analysis in target detection using a hyperspectral image from RIT (Rochester Institute of Technology). ROC curves and detector outputs are generated for the analysis. The image from RIT is shown in Fig. 1. The image is in the visible and near-infrared wavelengths and has spatial dimensions of 84 by 146 and a spectral dimension of 295. The two targets in the image are red felt and blue felt and are shown in Fig. 2. The mean target pixel used in both linear and quadratic discriminant detectors is the mean pixel from the simulated target pixels. The results presented in this section are for the red felt using the target spectra from the image. The results for the blue felt are similar to the red felt and are not shown.

Figure 1. The RIT image with spatial dimensions of 84 by 146 and spectral dimension of 295.

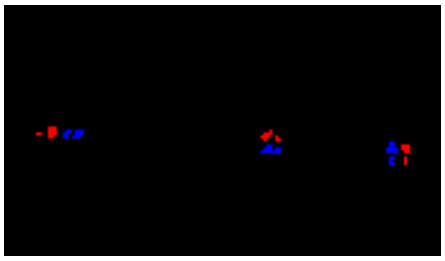

Figure 2. An image of the locations of the red and blue targets for the RIT image.

The linear discriminant detector in (13) requires only a sample of background pixels, but the quadratic discriminant detector in Equation (20) requires a sample of background pixels and a sample of target pixels. All pixels in the entire image are considered as background pixels although some of them are actually target pixels. All pixels from the image are selected as training pixels for background. It is assumed that there is only one target pixel in target detection so the mean of the target pixels is assumed to be the representative target pixel. A random sample of $3\times p$ pixels are generated from a uniform distribution to be used training pixels for target. Each training pixel for target is the sum of the mean target pixel and a scalar multiple of a random pixel from a uniform distribution that has the same magnitude as the mean target pixel. The scalar multiple is a proportion of the magnitude of the pixel and is denoted by q in percentage.

The ROC curves for the red target using the linear discriminant detector are shown in Fig. 3 for $q=1,2,\cdots,10$. The ROC curves for the red target using the quadratic discriminant detector are shown in Fig. 4 for $q=1,2,\cdots,10$. As the value of q increases, the ROC curve gets worse for linear and quadratic discriminant detectors. The linear discriminant detector performs best at $q=1$. The best ROC curves for the quadratic discriminant detector are at $q=1,2,3$. As more noise is introduced into the training pixels for the target, the performance of the linear discriminant detector gets progressively worse for the first three values of q but stays about the same after that. The performance of the quadratic discriminant detector stays about the same after the first four values of q. The roc curves show the

quadratic discriminant detector performs better than the linear discriminant detector for $q \geq 2$.

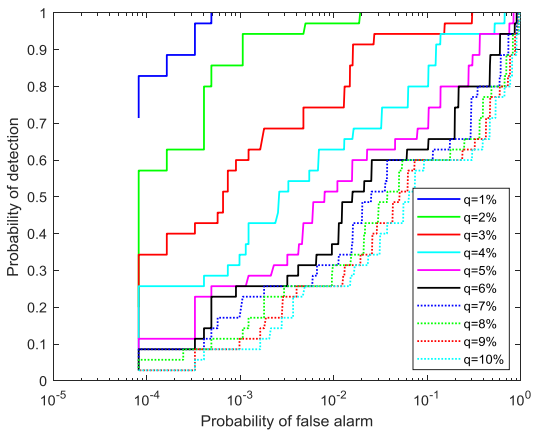

Figure 3. ROC curves generated by the linear discriminant detector for detecting the red target for q=1, 2, 3, …, 10.

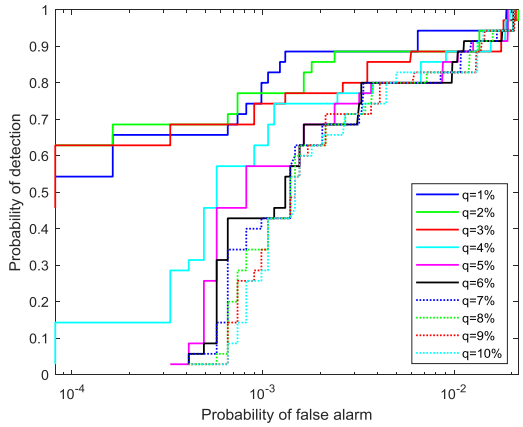

Figure 4. ROC curves generated by the quadratic discriminant detector for detecting the red target for q=1, 2, 3, …, 10.

The values of the detector are generated for analysis. The images of the detector output for the linear and quadratic discriminant detectors at $q=1$ are shown in Fig. 5 and Fig. 6. The image of the detector output for the AMF and ACE detectors are shown in Fig. 7 and Fig. 8. The detector images show that the detectors based on discriminant analysis can detect the red felt, but the background is a little noisy. The AMF and ACE detectors show rather homogeneous background. The red felt shows up more clearly in the ACE detector than in the AMF detector so the ACE detector performs better than the AMF detector.

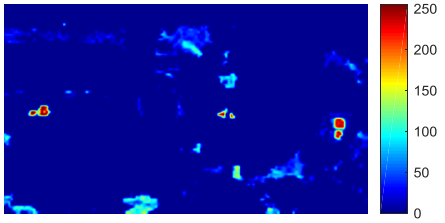

Figure 5. An image of the detector output generated by the linear discriminant detector at q=1 for detecting the red target.

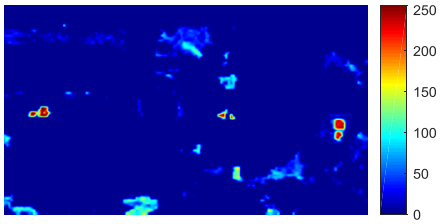

Figure 6. An image of the detector output generated by the quadratic discriminant detector at q=1 for detecting the red target.

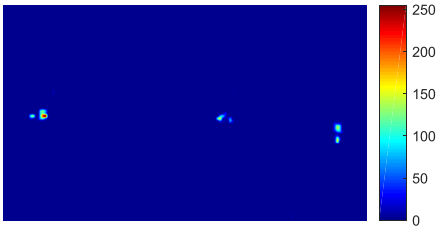

Figure 7. An image of the detector output generated by AMF detector for detecting the red target.

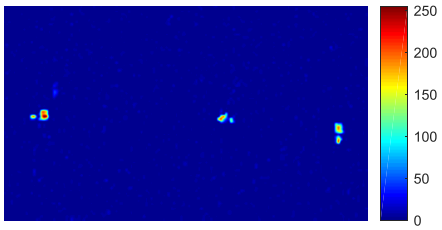

Figure 8. An image of the detector output generated by ACE detector for detecting the red target.

IV. Conclusion

The linear discriminant and quadratic discriminant detectors can detect the red felt using simulated target spectra that are generated with different amount of random noise. This shows that it is feasible to solve the target detection problem, which typically has only one training pixel for the target by using classification algorithms, which require a sample of training pixels for the target. Different methods of generating the simulated target pixels and different conventional classification algorithms can be combined develop new detectors for target detection.

Acknowledgment

The authors wish to thank the Center for Imaging Science, Rochester Institute of Technology, for the data.

References

[1] D. Manolakis and G. Shaw, "Detection algorithms for hyperspectral imaging applications," *IEEE Signal Processing Magazine*, vol. 19, pp. 29-43, 2002.

[2] S. Matteoli, M. Diani, and J. Theiler, "An overview background modeling for detection of targets and anomalies in hyperspectral remotely sensed imagery," *IEEE J. Sel. Topics in Applied Earth Observations and Remote Sensing*, vol. 7, pp. 2317-2336, 2014.

[3] S. Kraut and L. Scharf, "The CFAR adaptive sub-space detector is a scale-invariant GLRT," *IEEE Transaction Signal Processing*, vol. 47, pp. 2538-2541, 1999.
[4] S. Kraut, L. Scharf, and L. T. McWhorter, "Adaptive subspace detectors," *IEEE Trans. Signal Processing*, vol. 49, pp. 1-16, 2001.
[5] E. Truslow, D. Manolakis, M. Pieper, T. Cooley, and M. Brueggeman, "Performance prediction of matched filter and adaptive cosine estimator hyperspectral target detectors," *IEEE Journal of Selected Topics in Applied Earth Observations and Remote Sensing*, vol. 7, no. 6, pp. 2337-2349, 2014.
[6] E. Lo and I. Ientilucci, "Target detection in hyperspectral imaging using logistic regression," *Proc. of SPIE*, vol. 9840, no. 98400W, 2016.
[7] A. Zieman, J. Theiler, and I. Ientilucci, "Experiments with simplex ACE: Dealing with highly variable targets," *Proc. of SPIE*, vol. 10198, no. 101980F, 2017.
[8] A. Zieman and J. Theiler, "Simplex ACE: A constrained subspace detector," *Optical Engineering*, vol. 56, no. 8 (081808), pp. 1-13, 2017.
[9] E. J. Ientilucci, "Target detection assessment of the SHARE 2010/2012 hyperspectral data collection campaign," *Proc. SPIE*, vol. 9472, 2015.
[10] A. Schaum, "Enough with the additive target model," *Proc. SPIE*, vol. 9088, no. 90880C, 2014.
[11] S. Adler-Golden, J. Gruninger, and R. Sundberg, "Hyperspectral detection and identication with constrained target subspaces," in *Proc. IEEE International Geoscience and Remote Sensing Symposium*, 2008, pp. 465-468.

Edisanter Lo has a Ph.D. in Computational Mathematics from Arizona State University in Tempe (Arizona), an M.S. in Statistics from University of Arkansas in Fayetteville (Arkansas), and a B.S. in Electrical Engineering from Louisiana Tech University in Ruston (Louisiana).
He has been a faculty at Susquehanna University since 2001 and is a professor of mathematics and computer science. Prior to Susquehanna University, he worked as an associate research professional and in digital image processing to support ASU Planetary Geology Group's participation in several NASA and international robotic planetary missions for about 12 years. He also conducted research in several national research laboratories during his tenure at Susquehanna University.
His current publications include "Hyperspectral Anomaly Detection Based on Uniformly Partitioned Pixel" published in Pattern Analysis and Applications and "Partitioned Correlation Model for Hyperspectral Anomaly Detection" published in Optical Engineering. His current research interests include hyperspectral anomaly detection, hyperspectral target detection, machine learning, data science, artificial intelligence, and deep learning.